

Communication

Identification of Anti-TNF α VNAR Single Domain Antibodies from Whitespotted Bambooshark (*Chiloscyllium plagiosum*)

Linfei Zhao ^{1,2,†}, Mingliang Chen ^{2,3,†} , Xiaona Wang ⁴, Shoukai Kang ⁵, Weiwei Xue ^{4,*}  and Zengpeng Li ^{2,*}

¹ School of Fisheries and Life, Shanghai Ocean University, Shanghai 201306, China; zhaolinfei1996@outlook.com

² Key Laboratory of Marine Genetic Resources, State Key Laboratory Breeding Base of Marine Genetic Resources, Fujian Key Laboratory of Marine Genetic Resources, Fujian Collaborative Innovation Centre for Exploitation and Utilization of Marine Biological Resources, Third Institute of Oceanography Ministry of Natural Resources, Xiamen 361005, China; mlchen_gg@tio.org.cn

³ Co-Innovation Center of Jiangsu Marine Bio-Industry Technology, Jiangsu Ocean University, Lianyungang 222005, China

⁴ School of Pharmaceutical Sciences, Chongqing University, Chongqing 401331, China; 202029021021@cqu.edu.cn

⁵ Department of Biochemistry, Institute for Protein Design, University of Washington, Seattle, WA 98195, USA; kangsk@uw.edu

* Correspondence: xueww@cqu.edu.cn (W.X.); lizengpeng@tio.org.cn (Z.L.); Tel.: +86-592-2195393 (Z.L.)

† These authors have contributed equally to this work.

Abstract: Tumor necrosis factor α (TNF α), an important clinical testing factor and drug target, can trigger serious autoimmune diseases and inflammation. Thus, the TNF α antibodies have great potential application in diagnostics and therapy fields. The variable binding domain of IgNAR (VNAR), the shark single domain antibody, has some excellent advantages in terms of size, solubility, and thermal and chemical stability, making them an ideal alternative to conventional antibodies. This study aims to obtain VNARs that are specific for mouse TNF (mTNF) from whitespotted bamboosharks. After immunization of whitespotted bamboosharks, the peripheral blood leukocytes (PBLs) were isolated from the sharks, then the VNAR phage display library was constructed. Through phage display panning against mTNF α , positive clones were validated through ELISA assay. The affinity of the VNAR and mTNF α was measured using ELISA and Bio-Layer Interferometry. The binding affinity of 3B11 VNAR reached 16.7 nM. Interestingly, one new type of VNAR targeting mTNF was identified that does not belong to any known VNAR type. To understand the binding mechanism of VNARs to mTNF α , the models of VNARs-mTNF α complexes were predicted by computational modeling combining HawkDock and RosettaDock. Our results showed that four VNARs' epitopes overlapped in part with that of mTNFR. Furthermore, the ELISA assay shows that the 3B11 potentially inhibited mTNF α binding to mTNFR. This study may provide the basis for the TNF α blockers and diagnostics applications.

Keywords: whitespotted bambooshark; IgNAR; VNAR; single domain antibody; TNF α



Citation: Zhao, L.; Chen, M.; Wang, X.; Kang, S.; Xue, W.; Li, Z.

Identification of Anti-TNF α VNAR Single Domain Antibodies from Whitespotted Bambooshark (*Chiloscyllium plagiosum*). *Mar. Drugs* **2022**, *20*, 307. <https://doi.org/10.3390/md20050307>

Academic Editor: Se-Kwon Kim

Received: 30 March 2022

Accepted: 28 April 2022

Published: 29 April 2022

Publisher's Note: MDPI stays neutral with regard to jurisdictional claims in published maps and institutional affiliations.



Copyright: © 2022 by the authors. Licensee MDPI, Basel, Switzerland. This article is an open access article distributed under the terms and conditions of the Creative Commons Attribution (CC BY) license (<https://creativecommons.org/licenses/by/4.0/>).

1. Introduction

Owing to high affinity and specificity, monoclonal antibodies have been of common use for several decades for a plethora of biotechnological and biomedical applications [1–3]. However, their drawbacks, such as their large size (150 kDa) or cost-ineffective production, limit their application in underdeveloped areas [4–7]. In 1995, a novel immunoglobulin isotype, namely, the immunoglobulin new antigen receptor (IgNAR), was found in cartilaginous fish [8]. Like the heavy-chain antibody (HcAb) found in Camelidae (camels, llamas, and their relatives) [9], IgNAR is also a homodimer of IgH chains that do not associate with IgL chains [8]. There are also many subtle varieties in IgNAR among different species of sharks. In nurse sharks, the variable domain of the new antigen receptor (VNAR) is

joined to five constant (C1–C5) domains [10], while in whitespotted bamboo sharks, the C1 domain is spliced directly to C4 [11].

The VNAR domain, an Ig superfamily domain with four framework regions (FR1–4), has two β sheets associated together through two canonical cysteine residues in framework regions FR1 and FR3 [12,13]. In addition to framework regions, VNAR also contains two hypervariable regions (HVRs) and two complementarity-determining regions (CDRs), known as CDR1, hypervariable loop 2 (HV2), hypervariable loop 4 (HV4) and CDR3 [14,15], respectively. Besides these canonical cysteines, CDR3 can have one or two additional cysteines forming extra disulfide bridges within the VNAR domain. According to the position and number of non-canonical cysteines in the VNAR domain, IgNARs are classified into four types. Type I VNAR, which has only been found in nurse sharks (*Ginglymostoma cirratum*), possesses two non-canonical cysteine residues in CDR3 that form two disulfide bridges with FR2 and FR4 [8,16–18]. Type II VNAR contains the protruding CDR3, produced by a disulfide bridge formed between cysteine residues in CDR1 and CDR3 and possesses special paratopes that bind to pockets and grooves epitope [19–22]. Type III VNAR is similar to Type II, but with one highly conserved tryptophan residue in CDR1 positioned close to the disulfide bridge [16]. Unlike Type I–III VNARs, there is no non-canonical disulfide bond in Type IV [21,23].

Compared with conventional IgG, shark VNAR domains have advantageous properties due to their peculiar structure. First, sharks may generate high-affinity VNARs compared to conservative mammalian protein targets because of the evolutionary distance between mammals and sharks on the phylogenetic tree [24,25]. Second, the long CDR3 in sharks can access the buried epitopes or enzyme functional sites [24–27]. Third, VNARs may have good tissue penetration ability due to their small size [7,21]. Fourth, the structure of VNAR affords remarkable refolding properties after heat shock [28–31]. This makes them preferable in diagnostic applications and transport where heating may temporarily occur.

As a critically important inflammatory marker and drug target in sera, TNF α can be significantly induced after infection or injury via the activation of the immune cells [32,33]. On the one hand, TNF α plays a vital role in resolving infection and tissue repair through the signal transduction pathway [34]. On the other hand, sometimes, it may trigger a severe cytokine release storm that results in sepsis and autoimmune diseases, such as rheumatoid arthritis (RA), ankylosing spondylitis, psoriatic arthritis, and inflammatory bowel diseases (IBD) [35,36]. Until now, anti-TNF α monoclonal antibodies, soluble TNF α receptors with IgG chimeric protein, and anti-TNF α Fab fragments, which were used to block the bioactivity of TNF α in the inflammatory response, had become highly effective and powerful TNF α blocking agents in disease therapy [37–40]. Granted, each TNF α blocking strategy varies among studies in terms of both usefulness and effectiveness. The different intensity and tissue penetration achieved by different types of TNF α blockades may contribute to the variety of results. Furthermore, the cost of these agents remains a big challenge and limits their application in low-income families, primarily due to their large size, low expression level, and high immunogenicity [41].

Previous studies have isolated anti-TNF α , neutralizing VNARs through immunization of sharks [42–44]. However, there remains a significant requirement for new anti-TNF α blockades that may avoid or at least limit the drawbacks above. Extending diagnostic options for the growing clinical need is also desirable.

In this study, the mTNF recombinant protein was expressed and the whitespotted bambooshark was immunized with it. Then, an anti-mTNF α VNAR phage library was established through RT-PCR using mRNA from the whitespotted bambooshark PBLs. After the *in vitro* panning of the library against mTNF α antigens, 15 colonies of VNAR were identified. Interestingly, a new type of VNAR that targets mTNF was found. The 3B11 was expressed in the BL21 strain and ELISA and BLI were used to measure the affinity of 3B11. Additionally, the ELISA assay was used to test the 3B11 inhibition of TNF α -TNFR interaction. To better understand the mode of action, the 3D structures of VNARs

were predicted using AlphaFold2 [45] and their binding to mTNF α was modeled through protein–protein docking, combining HawkDock [46] and RosettaDock [47].

2. Results

2.1. Isolation and Characterization of mTNF α Specific VNAR from Whitespotted Bamboo Shark

To obtain anti-mTNF α VNAR single domain antibodies, the extracellular domain of mTNF α (mTNF α ECD,77-235aa) was purified as an antigen with high purity through the *E. coli* expression system (Figure 1a). Total RNA was extracted from the PBLs after immunization of two whitespotted bamboosharks with the mTNF α (ECD) protein. The VNAR encoding gene fragments were then amplified by PCR with about 400 bp fragments purified with gel extraction, which were then inserted into pComb3XSS vectors and electroporated into TG1 cells. After obtaining the Anti-mTNF α VNAR phage-displayed library, the library capacity and the insert ratio were then determined. The correct insert ratio was about 100% through the colony PCR assay, and the library capacity reached approximately 1×10^9 colony-forming units (CFU). Clone PCR analysis of 48 randomly chosen clones indicated that the percentage of the library insertion rate was 100% (Figure S1). Overall, these results indicate that an mTNF α -specific, phage-displayed VNAR library was successfully established.

Bio-panning was used to isolate mTNF-specific VNARs from a phage-displayed VNAR library. To evaluate the enrichment fold during phage display panning, the colony numbers among panning on mTNF α and non-fat milk as negative controls were compared. After two consecutive rounds of phage display bio-panning, the enrichment ratios of mTNF α -specific VNARs increased to about 260 times (Figure 1b). In addition, 63 positive clones with a binding ratio >5 were identified from a total of 96 randomly chosen clones by the phage-ELISA assay (Figure 1c). Then, the positive clones were sequenced, as shown in Figure 1d, and 15 anti-mTNF α VNARs with unique amino acid sequences were determined based on the sequencing analysis. Furthermore, these 15 anti-mTNF α VNARs were classified into 4 families based on the CDR3 amino acid sequences. Families 1–3 belong to type II VNAR. Interestingly, family 4 was a new type of VNAR that does not fit in any of the four known types (types I–IV). All 4 VNARs in family 4 possess one additional cysteine in the CDR3 domain but no cysteine in CDR1. In 1D11 VNAR, there is another cysteine in FR2. To further evaluate the species specificity of the VNARs, the human TNF α was expressed, and the phage ELISA was performed. As shown in Figure 1e, 3B7 and 3B11 could cross-react with human TNF α with weaker ELISA signals than mouse TNF α . However, 1D11 and 2F3 were specific for mouse TNF α , with no cross-reactivity toward human TNF α .

2.2. Expression of VNAR Single Domain Antibodies and 3B11 Antagonize the TNFR-TNF α Interaction

To determine the VNAR single-domain antibodies binding kinetics, the four typical anti-mTNF α VNARs, 1D11, 2F3, 3B7 and 3B11, were produced in *E. coli* BL21(DE3) strain. The expression yield of 3B11 is about 2.16 mg from 200 mL *E. coli* culture, whereas the other three VNARs are expressed at extremely low levels. Nickel-charged HisTrap columns were used to purify 3B11 VNAR proteins from the *E. coli* supernatants. Sodium dodecyl sulfate polyacrylamide gel electrophoresis (SDS-PAGE) analysis showed good quality with more than 90% purity after one-step purification (Figure 2a). To test whether 3B11 inhibits the TNF α –TNFR interaction, the ELISA assay was performed and the result shows that 3B11 can potentially block mTNFR binding to mTNF α (Figure 2b).

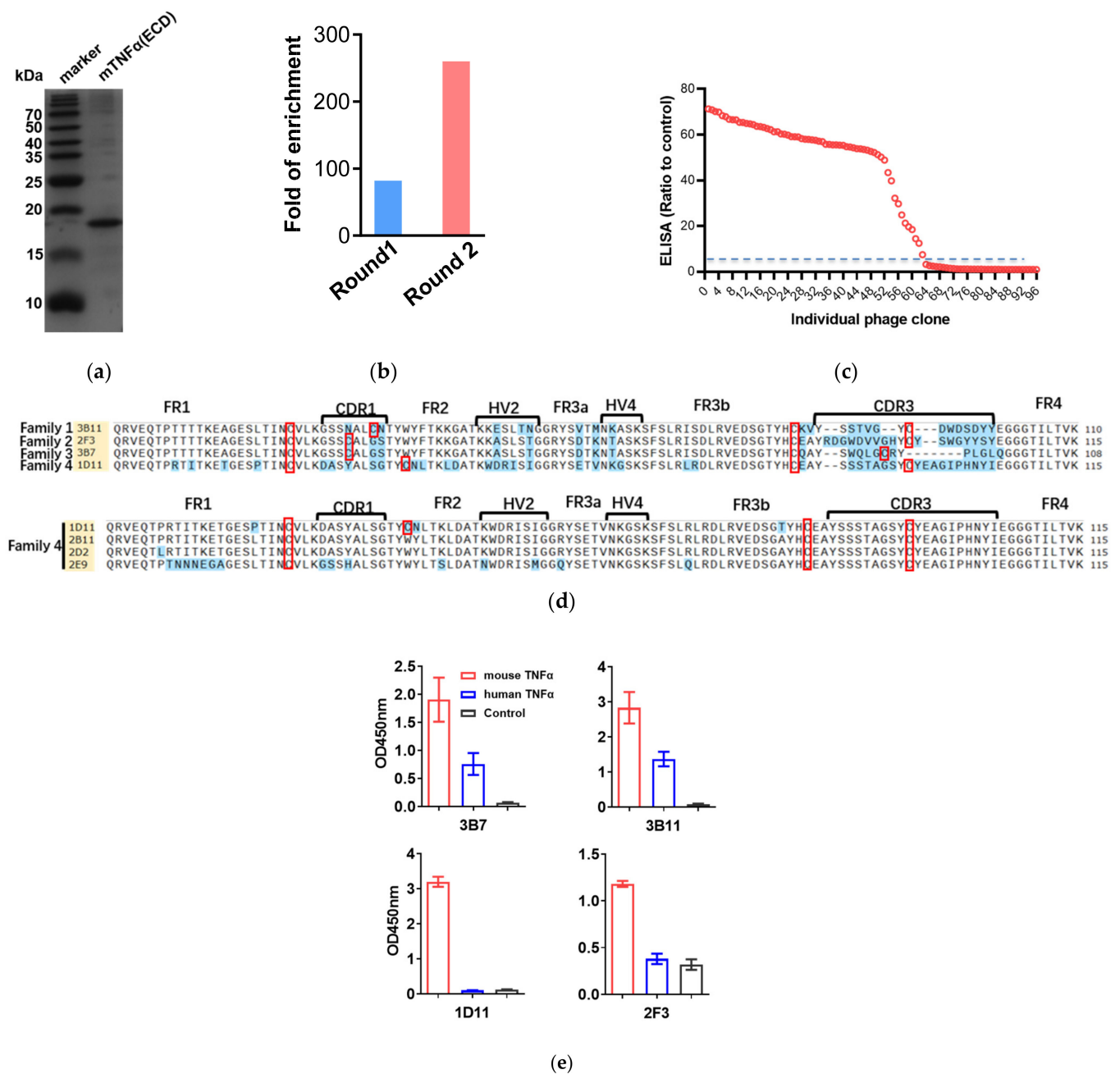


Figure 1. VNARs against mTNFα were selected by phage display panning. **(a)** SDS-PAGE analysis of mTNFα(ECD) purification by ProteinIso Ni-NTA resin. **(b)** The enrichment ratios of mTNFα-specific VNARs. **(c)** Independent clones (randomly picked from round 2) were tested for their ability to bind to mTNFα by phage display. 67% of the tested clones displayed a binding to mTNFα at least five times higher than their respective binding to non-fat milk. **(d)** Amino acid sequence alignment of anti-mTNFα VNARs. FR is framework region; CDR is complementarity-determining region; HV is hypervariable region. The Cys is indicated by a red box. **(e)** Cross-reactivity between four typical VNARs and hTNFα was detected by phage ELISA.

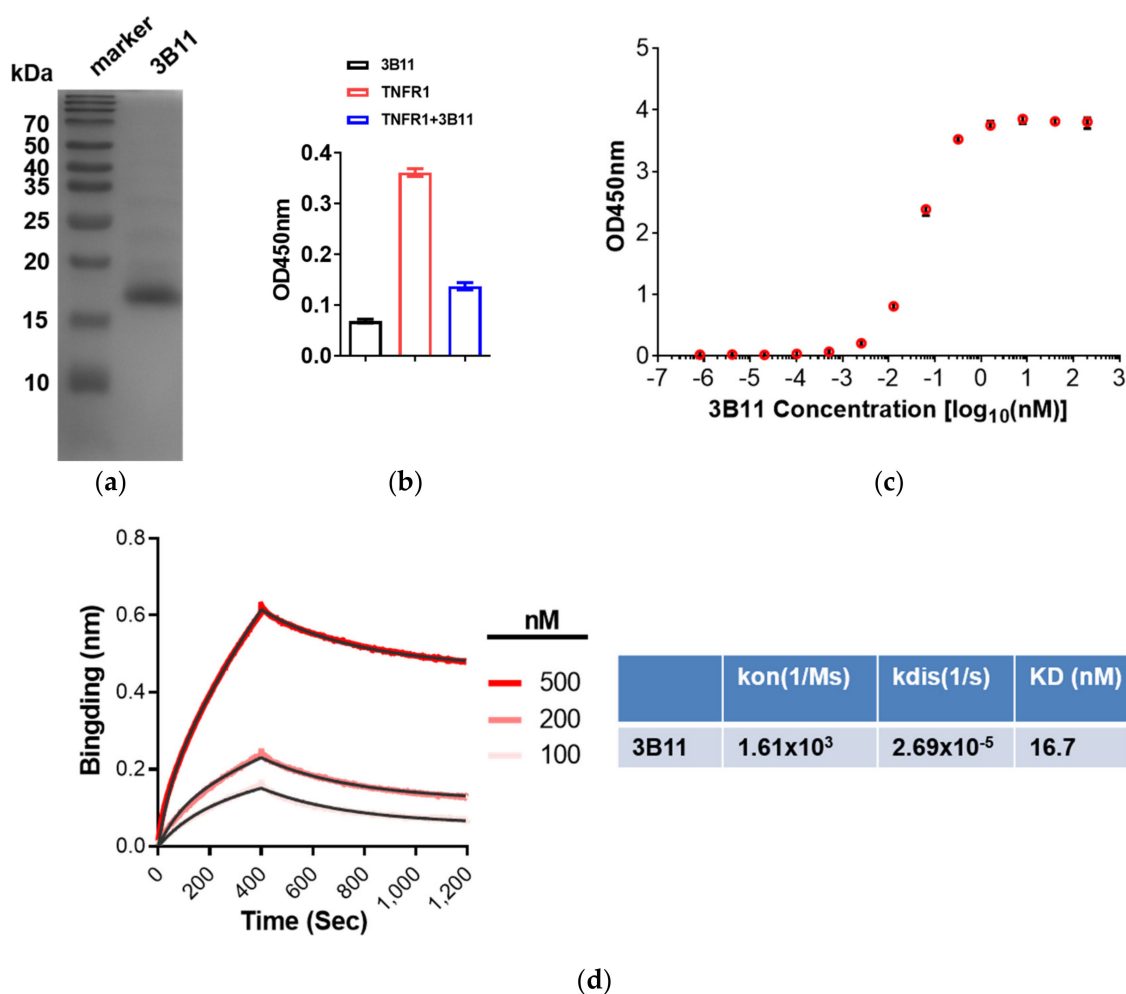


Figure 2. The binding affinity test of 3B11 VNAR and mTNF α . (a) SDS-PAGE and Coomassie blue staining of anti-TNF α 3B11 VNAR purification. (b) 3B11 VNAR potentially blocked TNFR binding to TNF α by ELISA. (c) Binding affinities of anti-mTNF α 3B11 VNAR toward the mTNF α , as determined by ELISA. (d) Kinetics of the mTNF α -VNAR interaction determined by an Octet K2 BLI Analysis System.

2.3. Affinity Assay of Anti-mTNF α 3B11 VNAR

To measure the affinity of the 3B11 VNAR with mTNF α , the ELISA and BLI experiments were performed. The ELISA EC₅₀ value of 3B11 VNAR was 0.36 nM (Figure 2c). However, through the BLI assay, 3B11 had 16.7 nM KD binding affinity for mTNF α , which was much lower than the affinity tested by the ELISA result (Figure 2c,d). During the BLI assay, the SA biosensors were used to capture the biotin-labeled mTNF α through the biotin-NHS-biotinylation labeling reaction, which may cause the instability of the protein or the steric effect between mTNF α and VNAR.

2.4. Models of VNARs-mTNF α Complexes

In this work, the ideal docking funnels of the four VNARs binding to mTNF α were obtained (Figure 3). For each complex, the structure with the lowest I-sc and I-rmsd ≤ 4 Å from the docking trajectory was selected for further analysis. As shown in Figure 3, 1D11, 2F3, 3B7 and 3B11 attach to the concave surface of mTNF α . To further understand the mechanism of action, the structure of mTNF α in complex with mTNFR was constructed using the hTNF α -hTNFR complex structure [48] as a reference. As a result, Figure 4 shows that all four VNARs' epitopes overlapped in part with that of mTNFR. In detail, 1D11 occupies the bottom of the receptor's binding area on mTNF α (Figure 4a), and 2F3, 3B7

and 3B11 occupy the central area of the receptor's binding area on mTNF α (Figure 4b). However, 3B7 has the largest overlapped area with the receptor compared to other VNARs.

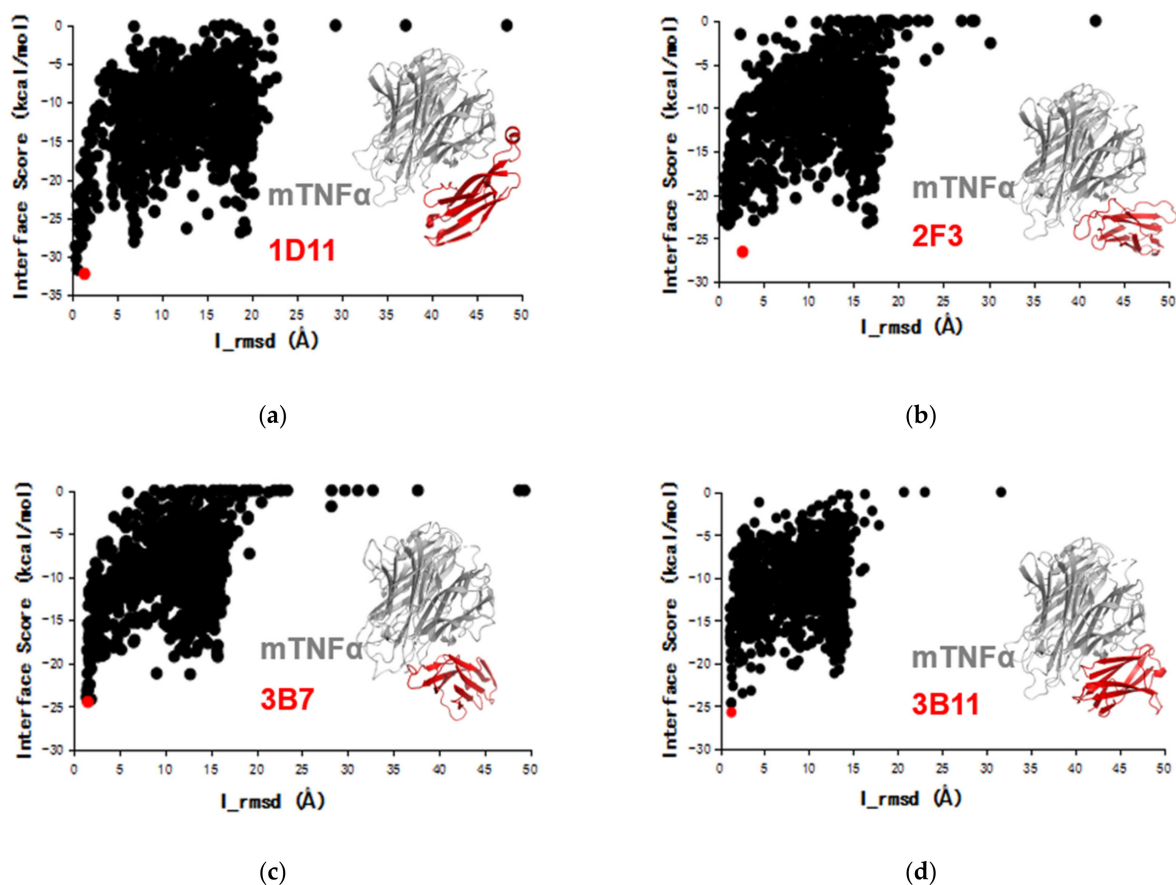


Figure 3. The Rosetta docking funnels of four VNARs 1D11, 2F3, 3B7 and 3B11 to mTNF α (a–d). The red plots have the lowest docking interface score (I-sc) with the interface root-mean-square deviation (I_{rmsd}) $\leq 4 \text{ \AA}$. Inset: TNF trimer (gray) and VNARs (red).

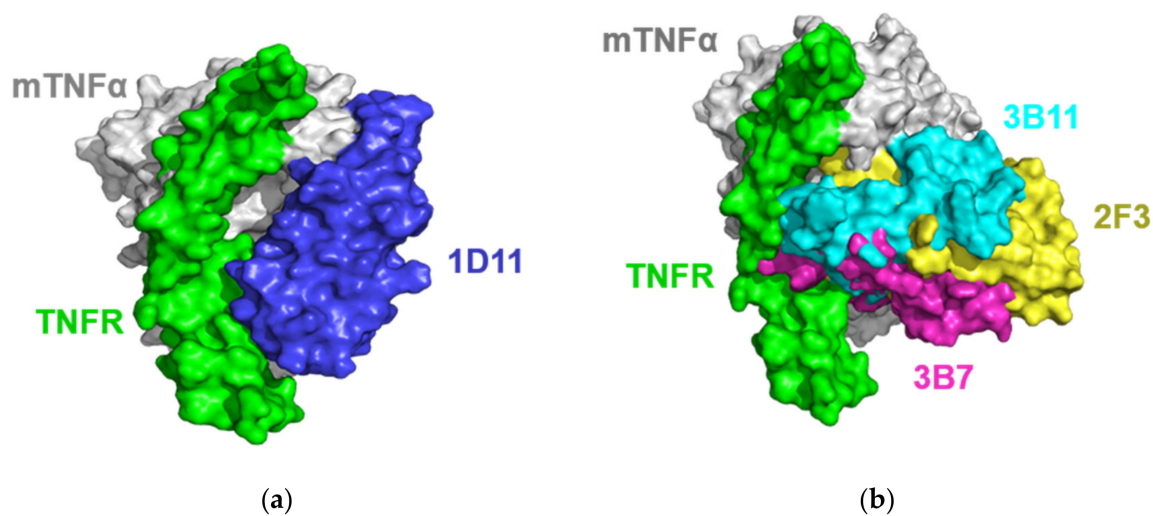


Figure 4. Surface representation of the four VNARs and the mTNFR (PDB ID: 6MKZ) on mTNF α . (a) 1D11 (blue) and mTNFR (green) on mTNF α (gray). (b) 2F3 (yellow), 3B7 (magenta), 3B11 (cyan) and mTNFR (green) on mTNF α (gray).

3. Discussion

The whitespotted bamboo shark is a member of the hemiscyllidae family of sharks, which is commonly found in the coral reefs of the Pacific Ocean. They are widely distributed in the coastal areas of southeastern China and surrounding waters and are also used for human consumption. Previously, the nurse shark was the most commonly used shark species for immunization and VNAR preparation. Comparably, the whitespotted bambooshark, which is relatively small and easy to keep, is an attractive alternative animal model to study and obtain specific antigen VNARs through immunization. In this study, the mouse TNF α protein was used to immunize whitespotted bamboosharks. Previously, many studies combined subcutaneous and intravenous administration for shark immunization in different sharks [49–52]. In this work, whitespotted bamboosharks were immunized following the subcutaneous and intravenous administration immunization protocol. TNF α -specific VNARs were obtained through phage display panning, which indicated that the immunization protocol is effective for high-affinity VNAR isolation in whitespotted bamboosharks.

However, after immunization, there was no secondary antibody available for the IgNAR from whitespotted bamboosharks. The commercial horn shark IgNAR antibody from GeneTex (GTX128445) was tested through Western blot and ELISA, but this IgNAR antibody does not work for the IgNAR from whitespotted bamboosharks. In the future, the secondary antibodies/nanobodies targeting IgNAR from whitespotted bamboosharks, which make it feasible to test the IgNAR titer in whitespotted bamboosharks, will be required.

Single-domain antibodies are becoming a promising tool both in diagnostics and therapeutic applications. In this study, the mTNF α VNARs were isolated through immunization of whitespotted bamboosharks and phage display panning. Among the VNAR sequences, a very special VNAR type was identified. In this new kind of VNAR, 1D11 has two non-canonical cysteine residues in FR2 and CDR3, but through the AlphaFold2 prediction, the two cysteines do not form a disulfide bridge. There is only one non-canonical cysteine in the other 3 members of this type of VNAR. To the best of our knowledge, this is the first report on this kind of VNAR that targets specific antigen, and more studies are needed to clarify the characteristics of this new kind of VNAR—for example, the epitope, thermostability, affinity and so on.

In this research, the affinity of the VNAR 3B11 was measured through ELISA and BLI, both of which show that 3B11 has a high affinity to mTNF α . Moreover, the molecular mimicry of anti-mTNF α VNARs indicate that all the four typical VNARs bind to the mTNF α epitopes that partially overlapped with TNFR, which means that all the VNARs may be potential mTNF α blocking agents. So, these mTNF α potential binders may be very good tools for the research of TNF α in the mouse model.

4. Materials and Methods

4.1. Ethics Statement

All procedures were approved by the Animal Care and Use Committee of the Third Institute of Oceanography, Ministry of Natural Resources, and conformed to the guidelines of the Fujian Provincial Department of Science and Technology for the Administration of Affairs Concerning Experimental Animals.

4.2. mTNF α Protein Expressing

The mTNF α (77-235 aa) DNA sequence was cloned into a pET-28a (+) vector using *Bam*HI and *Xho*I restriction enzymes (Takara, Beijing, China). The plasmid was transformed into *Escherichia coli* BL21 (DE3) cells and plated on LB-Agar (1% tryptone, 0.5% yeast extract, 1% NaCl, 1.5% agar) with 30 μ g/mL Kanamycin sulfate at 37 °C overnight. Single colonies were selected and cultured in LB media. When OD600 reached 0.4–0.6, the culture was induced with 1 mM IPTG and incubated at 30 °C for 16 h. Cells were harvested and washed twice with a PBS buffer (Sangon, Biotech, Shanghai, China). Then, the cells were lysed by Ultrasonic machining in a lysis buffer (25 mM Tris, 150 mM NaCl, 1 mM

PMSF, 1 mg/mL lysozyme, 10% glycerol, pH 7.5). Protein extracts were collected by centrifugation at 12,000 rpm for 30 min. The mTNF α containing His-tag was purified by ProteinIso Ni-NTA resin (TransGen Biotech, Beijing, China) and natively eluted with a different imidazole buffer (25 mM Tris, 150 mM NaCl, 25–500 mM imidazole, 10% glycerol, pH 7.5). The eluted mTNF α protein was subsequently dialyzed with a dialysis buffer (1 \times PBS, pH 7.5), and a portion of the mTNF α protein was treated by thrombin protease overnight to remove His-tag.

4.3. Immunization of Whitespotted Bamboo Sharks

Briefly, as shown in Table 1, two whitespotted bamboo sharks weighing about 0.5 kg were immunized, according to the protocol modified from previous studies. The mTNF α protein was emulsified in equal amounts of adjuvant (CFA (complete Freund's adjuvant) or IFA (incomplete Freund's adjuvant)) and subcutaneously injected in the pectoral fin as a mixed antigen cocktail. Subsequent boosts were administered intravenously in the caudal vein. Two weeks after the fourth immunization, the sharks' PBLs were isolated to construct an immune VNAR library.

Table 1. Schedule for immunization of whitespotted bamboo sharks with mTNF α .

Week Number	Procedure	Details	Immunization Route
0	Immunization 1	200 μ g mTNF α in CFA	Subcutaneous
4	Immunization 2	200 μ g mTNF α in IFA	Subcutaneous
8	Immunization 3	100 μ g mTNF α soluble	Intravenous
12	Immunization 4	100 μ g mTNF α soluble	Intravenous

The whitespotted bamboo sharks were comfortably housed at the Third Institute of Oceanography, Ministry of Natural Resources, and were anesthetized with MS-222 (Sigma, St. Louis, MO, USA) at approximately 0.1% (*w/v*) in artificial seawater before any procedure.

4.4. VNAR Library Construction

By the TRIZOL method, total mRNA was extracted from the purified PBLs and the concentration was measured by optical density at 260 nm. Then, cDNA was synthesized using PrimeScriptTM II 1st Strand cDNA Synthesis Kit (Takara, Beijing, China). The VNAR fragments were obtained after PCR amplification of the cDNA by PCR using specific primers (Table 2). The PCR products corresponding to VNAR genes were analyzed by agarose gel electrophoresis. At the same time, the PCR products were digested with the SfiI restriction enzyme (NEB, Ipswich, New England), then inserted into the phagemid pComb3XSS with T4 ligase (Thermo Scientific, Waltham, MA, USA). By electroporation, recombinant plasmids were transformed into *E. coli* TG1 cells and plated onto 2 \times YT-Agar (1.6% tryptone, 1% yeast extract, 0.5% NaCl, 1.5% agar, 1% glucose) containing 100 μ g/mL ampicillin and cultured at 37 $^{\circ}$ C overnight.

Table 2. Details of primers used in the PCR experiment. SfiI restriction enzyme sites are underlined.

Primer	Sequence
VNAR-1- Forward	TCGCTACCGT <u>ggcccaggcggcc</u> CAACGGGTTGAACAAACACC
VNAR-2- Forward	TCGCTACCGT <u>ggcccaggcggcc</u> GCATGGGTTGAGCAAACACCC
VNAR-1- Reverse	TGATGGTGCT <u>ggccggcctggcc</u> TTTCACAGTCAGAATGGTGC
VNAR-2- Reverse	TGATGGTGCT <u>ggccggcctggcc</u> TTTCACTGTTAGAAAAGTGCC

4.5. Selection of TNF α -Specific VNAR by Phage ELISA

The Immuno-tubes (Thermo Scientific, Waltham, MA, USA) coated with 5 mL of mTNF α with respective concentrations of 100 μ g/mL (Round 1) and 50 μ g/mL (Round 2)

were incubated overnight at 4 °C. After washing and blocking by 5% Not-fat Powdered Milk (Sangon Biotech, Shanghai, China), 100 µL of the amplified phage display library (3.54×10^{13} pfu/mL) was added to each immune-tube and incubated for 1 h at room temperature in a rotator. The unbound phage was removed by washing 3 times with PBST (PBS, 0.1% Tween-20) in Round 1. The number of washes was increased to 6 times for subsequent rounds of panning. Two rounds of panning were performed. Phagemid particles were eluted using 0.1 M HCl, which was neutralized by adding 1 M Tris-base, and immediately reinfected with *E. coli* TG1. After 1 h of incubation on a shaker, the cell was plated onto a 2 × YT containing 1% glucose and 100 µg/mL ampicillin and cultured at 37 °C overnight.

A total of 96 *E. coli* clones were randomly selected, and the phage supernatant containing the VNAR fragments were obtained by the phage display technique. The mTNFα was dissolved in a PBS buffer at 10 µg/mL to coat 96-well plates, 100 µL/well, at 4 °C overnight. The irrelevant antigen used was 5 µg/mL BSA in PBS. After the plate was blocked with 5% Non-fat Powdered Milk in the PBS buffer, 100 µL phage supernatant was added to the plate. Binding was detected by an HRP conjugated mouse anti-M13 antibody (Sino Biological, Beijing, China). The cut-off value for the positive binder was set as a 5× higher signal compared to the control.

4.6. Soluble VNAR Production and Purification

According to the DNA sequencing results, VNAR binder sequences were cloned into a pET-28a (+) and were transformed into *E. coli* BL21 (DE3) cells. The form colonies were pooled in 500 mL LB media containing 30 µg/mL Kanamycin at 37 °C until the OD₆₀₀~0.4–0.6. The culture was induced with 0.1 mM IPTG and incubated at 16 °C overnight for soluble protein production. Bacteria pellets were spun down and resuspended in 30 mL of ice-cold lysis buffer. The cell suspension was incubated on ice for 30 min. Cells were ultrasound broken on ice. The slurry was then centrifuged at 12,000 rpm for 30 min at 4 °C. Soluble VNAR containing His-tags was purified from the cell lysate by Ni-NTA resin and finally used different density imidazole buffers to elute VNAR protein.

4.7. ELISA for VNAR Affinity Detection

Antigens were coated onto a 96-well ELISA plate (NEST, Wuxi, China) at an amount of approximately 100 ng per well in the PBS buffer overnight at 4 °C. The well surface was then blocked with a blocking buffer (PBS, 5% Not-fat Powdered Milk) at 37 °C for 2 h. Antigens coated reference 4.7. For the VNAR affinity test, the scramble VNAR that does not bind the mTNFα was used for negative controls. The VNAR was serially 5-fold dilution from 1 µM to 0.8192 fM in the blocking buffer. After 2 h of incubation with VNAR at room temperature, His-tag mAb (Bioword, Nanjing, China) was diluted at 1:1000 and incubated for 2 h at room temperature again. Then, the goat anti-mouse IgG (Abclonal, Wuhan, China) was diluted at 1:5000 and incubated for 1 h at room temperature. Nine washes with PBST were carried out between each incubation to remove nonspecific absorbances. After the final wash, the samples were further incubated in dark with a freshly prepared TMB Single-Component Substrate solution (Solarbio, Beijing, China) for 10 min at room temperature to develop the signals. After the stop solution (92 mM H₂SO₄), the plates were read at 450 nm on a plate reader. The raw data were processed by Prism 7i (GraphPad, San Diego, CA, USA) to calculate EC₅₀. For 3B11 blocking TNFα-TNFR interaction assay, mTNFα were coated onto a 96-well ELISA plate, then 50 µL TNFRSF1AhFc (20 ng/mL, Sino Biological, Beijing, China, Cat:50496-M02H) and 50 µL 3B11 (3 µM) was successively added to the wells. Control wells were added with 100 µL using 5% milk in PBST. After a 2 h incubation, the Goat Anti-Human IgG Fc (HRP) (Abcam, Cambridge, UK) was diluted at 1:5000 and incubated for 1 h at room temperature. The following procedure is the same as above.

4.8. BLI-Based Affinity Assay

BLI-based mTNF α binding inhibition experiments were carried out by BLI using an Octet K2 Protein Analysis System. The measurements were performed using Streptavidin (SA) biosensors. In brief, the mTNF α proteins were immobilized onto the SA biosensor surface via biotin (biotin-NHS)-biotinylation (MCE, Shanghai, China) labeling reaction, following the manufacturer's directions. The mTNF α proteins were labeled with biotin at a concentration of 1 μ M for half an hour and dialyzed with PBS at 4 °C overnight. All steps were performed at room temperature, with a working volume of 200 μ L in each well. The mTNF α antigen–antibody basic kinetic experiments were made up of baseline (PBST, 1 \times PBS + 0.02% tween-20, 60 s); mTNF α protein loading (2 μ g/mL mTNF α , PBST, pH7.4, 300 s); baseline2 (PBST, 120 s); 500 nM, 250 nM, 100 nM, 50 nM anti-mTNF α VNAR association (anti-mTNF α VNAR, PBST, 400 s); and dissociation (PBST, 800 s). For the control sample, the same amount of PBST buffer was added to the mTNF α sample to remove the interference from the PBST buffer itself. The response data were normalized using Octet data analysis studio 12.2 (Sartorius, Goettingen, Germany).

4.9. Computational Modeling

For each VNAR, the multiple sequence alignment file was first generated using MMseqs2 [53]. Then, the 3D structures of 3B7, 3B11, 1D11 and 2F3 were predicted by AlphaFold2 [45], and the top-ranked models with high pLDDT were selected as their 3D structures.

Based on the predicted 3D structures of VNARs and the crystal structure of mTNF α (PDB ID: 2TNF [54]), the binding modes between VNARs and mTNF α were obtained by using the protein–protein docking strategy combining HawkDock [46] and RosettaDock [47]. First, HawkDock [46] was performed to preliminarily explore the poses of each VNAR and TNF α , which generated the top 10 prediction complex models. Referring to the binding epitopes of Nanobodies on human TNF α [48], 5 reasonable models were then selected for RosettaDock using the same setup as recent studies [55,56]. In brief, the initial model was prepacked and used as a starting point for several rounds of local docking to generate 1000 decoys by running RosettaDock with the Monte Carlo (MC) refinement method [57]. Finally, the docking funnel of the trajectory describing the characteristics of the interface score (I-sc) of each decoy and the interface root-mean-square deviation (I_rmsd) was made to find the reasonable model of each complex [55,56,58].

4.10. Statical Analyses

For the biopanning and ELISA assays, data were analyzed using GraphPad Prism 7 (GraphPad, San Diego, CA, USA).

5. Conclusions

In this study, the ability to raise the specific IgNAR from whitespotted bamboosharks against mTNF α by immunization was demonstrated. After immunization, a phage display VNAR library was successfully constructed by PCR amplification. Selection from this phage display VNAR library resulted in 15 unique clones with specificity for mTNF α , suggesting that the enrichment of affinity VNARs against mTNF α proteins has been successfully achieved through iterative biopanning. Interestingly, one new type of VNAR targeting mTNF α that does not belong to any known VNAR type was identified. Additionally, 3B11 VNAR was expressed in *E. coli* and the binding affinity of 3B11 VNAR reached 16.7 nM through the BLI assay. The models of VNARs–mTNF α complexes were predicted by computational modeling combining HawkDock and RosettaDock. The results indicated that the four VNARs' epitopes overlapped in part with that of mTNFR.

Supplementary Materials: The following supporting information can be downloaded at: <https://www.mdpi.com/article/10.3390/md20050307/s1>. Figure S1: The PCR verified the library quality.

Author Contributions: Z.L. conceptualized this research. L.Z. performed VNAR screening and biochemically characterized VNAR candidates; M.C. performed the immunization of sharks; X.W. and W.X. performed the molecular mimicry. S.K. analyzed the BLI data. Z.L., L.Z. and W.X. wrote the manuscript with the assistance from other authors. All authors have read and agreed to the published version of the manuscript.

Funding: This work was supported by grants from the Scientific Research Foundation of Third Institute of Oceanography, SOA (2018016), Excellent Youth Foundation of Fujian Scientific Committee (2018J06011), Outstanding Young Talent Project, the Ministry of Natural Resources of China (No. 1211060000018003927) and Deep-Sea Habitats Discovery Project (DY-XZ-04).

Institutional Review Board Statement: All procedures were approved by the Animal Care and Use Committee of the Third Institute of Oceanography, Ministry of Natural Resources, and conformed to the guidelines of the Fujian Provincial Department of Science and Technology for the Administration of Affairs Concerning Experimental Animals.

Acknowledgments: We thank all members of Li lab for their helpful comments.

Conflicts of Interest: A provisional patent related to this work has been filed by the Third Institute of Oceanography Ministry of Natural Resources.

References

1. Weiner, L.M.; Murray, J.C.; Shuptrine, C.W. Antibody-based immunotherapy of cancer. *Cell* **2012**, *148*, 1081–1084. [[CrossRef](#)] [[PubMed](#)]
2. Leow, C.H.; Fischer, K.; Leow, C.Y.; Cheng, Q.; Chuah, C.; McCarthy, J. Single Domain Antibodies as New Biomarker Detectors. *Diagnostics* **2017**, *7*, 52. [[CrossRef](#)] [[PubMed](#)]
3. Belanger, K.; Iqbal, U.; Tanha, J.; MacKenzie, R.; Moreno, M.; Stanimirovic, D. Single-Domain Antibodies as Therapeutic and Imaging Agents for the Treatment of CNS Diseases. *Antibodies* **2019**, *8*, 27. [[CrossRef](#)] [[PubMed](#)]
4. Qiu, X.Q.; Wang, H.; Cai, B.; Wang, L.L.; Yue, S.T. Small antibody mimetics comprising two complementarity-determining regions and a framework region for tumor targeting. *Nat. Biotechnol.* **2007**, *25*, 921–929. [[CrossRef](#)] [[PubMed](#)]
5. Chames, P.; Van Regenmortel, M.; Weiss, E.; Baty, D. Therapeutic antibodies: Successes, limitations and hopes for the future. *Br. J. Pharmacol.* **2009**, *157*, 220–233. [[CrossRef](#)] [[PubMed](#)]
6. Hansel, T.T.; Kropshofer, H.; Singer, T.; Mitchell, J.A.; George, A.J. The safety and side effects of monoclonal antibodies. *Nat. Rev. Drug Discov.* **2010**, *9*, 325–338. [[CrossRef](#)]
7. Mordenti, J.; Cuthbertson, R.A.; Ferrara, N.; Thomsen, K.; Berleau, L.; Licko, V.; Allen, P.C.; Valverde, C.R.; Meng, Y.G.; Fei, D.T.; et al. Comparisons of the intraocular tissue distribution, pharmacokinetics, and safety of 125I-labeled full-length and Fab antibodies in rhesus monkeys following intravitreal administration. *Toxicol. Pathol.* **1999**, *27*, 536–544. [[CrossRef](#)]
8. Greenberg, A.S.; Avila, D.; Hughes, M.; Hughes, A.; McKinney, E.C.; Flajnik, M.F. A new antigen receptor gene family that undergoes rearrangement and extensive somatic diversification in sharks. *Nature* **1995**, *374*, 168–173. [[CrossRef](#)]
9. Hamers-Casterman, C.; Atarhouch, T.; Muyldermans, S.; Robinson, G.; Hamers, C.; Songa, E.B.; Bendahman, N.; Hamers, R. Naturally occurring antibodies devoid of light chains. *Nature* **1993**, *363*, 446–448. [[CrossRef](#)]
10. Greenberg, A.S.; Hughes, A.L.; Guo, J.; Avila, D.; McKinney, E.C.; Flajnik, M.F. A novel “chimeric” antibody class in cartilaginous fish: IgM may not be the primordial immunoglobulin. *Eur. J. Immunol.* **1996**, *26*, 1123–1129. [[CrossRef](#)]
11. Zhang, W.; Qin, L.; Cai, X.; Juma, S.N.; Xu, R.; Wei, L.; Wu, Y.; Cui, X.; Chen, G.; Liu, L.; et al. Sequence structure character of IgNAR Sec in whitespotted bamboo shark (*Chiloscyllium plagiosum*). *Fish Shellfish Immunol.* **2020**, *102*, 140–144. [[CrossRef](#)] [[PubMed](#)]
12. Zielonka, S.; Empting, M.; Grzeschik, J.; Konning, D.; Barelle, C.J.; Kolmar, H. Structural insights and biomedical potential of IgNAR scaffolds from sharks. *MAbs* **2015**, *7*, 15–25. [[CrossRef](#)] [[PubMed](#)]
13. Feng, M.; Bian, H.; Wu, X.; Fu, T.; Fu, Y.; Hong, J.; Fleming, B.D.; Flajnik, M.F.; Ho, M. Construction and next-generation sequencing analysis of a large phage-displayed VNAR single-domain antibody library from six naive nurse sharks. *Antib. Ther.* **2019**, *2*, 1–11. [[CrossRef](#)] [[PubMed](#)]
14. Dooley, H.; Stanfield, R.L.; Brady, R.A.; Flajnik, M.F. First molecular and biochemical analysis of in vivo affinity maturation in an ectothermic vertebrate. *Proc. Natl. Acad. Sci. USA* **2006**, *103*, 1846–1851. [[CrossRef](#)]
15. Zielonka, S.; Weber, N.; Becker, S.; Doerner, A.; Christmann, A.; Christmann, C.; Uth, C.; Fritz, J.; Schafer, E.; Steinmann, B.; et al. Shark Attack: High affinity binding proteins derived from shark vNAR domains by stepwise in vitro affinity maturation. *J. Biotechnol.* **2014**, *191*, 236–245. [[CrossRef](#)]
16. Diaz, M.; Stanfield, R.L.; Greenberg, A.S.; Flajnik, M.F. Structural analysis, selection, and ontogeny of the shark new antigen receptor (IgNAR): Identification of a new locus preferentially expressed in early development. *Immunogenetics* **2002**, *54*, 501–512. [[CrossRef](#)]
17. Kovaleva, M.; Johnson, K.; Steven, J.; Barelle, C.J.; Porter, A. Therapeutic Potential of Shark Anti-ICOSL VNAR Domains is Exemplified in a Murine Model of Autoimmune Non-Infectious Uveitis. *Front Immunol.* **2017**, *8*, 1121. [[CrossRef](#)]

18. Fennell, B.J.; Darmanin-Sheehan, A.; Hufton, S.E.; Calabro, V.; Wu, L.; Muller, M.R.; Cao, W.; Gill, D.; Cunningham, O.; Finlay, W.J. Dissection of the IgNAR V domain: Molecular scanning and orthologue database mining define novel IgNAR hallmarks and affinity maturation mechanisms. *J. Mol. Biol.* **2010**, *400*, 155–170. [[CrossRef](#)]
19. Streltsov, V.A.; Carmichael, J.A.; Nuttall, S.D. Structure of a shark IgNAR antibody variable domain and modeling of an early-developmental isotype. *Protein Sci.* **2005**, *14*, 2901–2909. [[CrossRef](#)]
20. Roux, K.H.; Greenberg, A.S.; Greene, L.; Strelets, L.; Avila, D.; McKinney, E.C.; Flajnik, M.F. Structural analysis of the nurse shark (new) antigen receptor (NAR): Molecular convergence of NAR and unusual mammalian immunoglobulins. *Proc. Natl. Acad. Sci. USA* **1998**, *95*, 11804–11809. [[CrossRef](#)]
21. Streltsov, V.A.; Varghese, J.N.; Carmichael, J.A.; Irving, R.A.; Hudson, P.J.; Nuttall, S.D. Structural evidence for evolution of shark Ig new antigen receptor variable domain antibodies from a cell-surface receptor. *Proc. Natl. Acad. Sci. USA* **2004**, *101*, 12444–12449. [[CrossRef](#)] [[PubMed](#)]
22. Stanfield, R.L.; Dooley, H.; Verdino, P.; Flajnik, M.F.; Wilson, I.A. Maturation of shark single-domain (IgNAR) antibodies: Evidence for induced-fit binding. *J. Mol. Biol.* **2007**, *367*, 358–372. [[CrossRef](#)] [[PubMed](#)]
23. Muller, M.R.; Saunders, K.; Grace, C.; Jin, M.; Piche-Nicholas, N.; Steven, J.; O'Dwyer, R.; Wu, L.; Khetemenee, L.; Vugmeyster, Y.; et al. Improving the pharmacokinetic properties of biologics by fusion to an anti-HSA shark VNAR domain. *MAbs* **2012**, *4*, 673–685. [[CrossRef](#)] [[PubMed](#)]
24. Nuttall, S.D.; Walsh, R.B. Display scaffolds: Protein engineering for novel therapeutics. *Curr. Opin. Pharmacol.* **2008**, *8*, 609–615. [[CrossRef](#)] [[PubMed](#)]
25. Barelle, C.; Gill, D.S.; Charlton, K. Shark novel antigen receptors—The next generation of biologic therapeutics? *Adv. Exp. Med. Biol.* **2009**, *655*, 49–62. [[CrossRef](#)]
26. Wesolowski, J.; Alzogaray, V.; Reyelt, J.; Unger, M.; Juarez, K.; Urrutia, M.; Cauerrhff, A.; Danquah, W.; Rissiek, B.; Scheuplein, F.; et al. Single domain antibodies: Promising experimental and therapeutic tools in infection and immunity. *Med. Microbiol. Immunol.* **2009**, *198*, 157–174. [[CrossRef](#)]
27. Ho, M. Inaugural Editorial: Searching for Magic Bullets. *Antib. Ther.* **2018**, *1*, 1–5. [[CrossRef](#)]
28. Dooley, H.; Flajnik, M.F.; Porter, A.J. Selection and characterization of naturally occurring single-domain (IgNAR) antibody fragments from immunized sharks by phage display. *Mol. Immunol.* **2003**, *40*, 25–33. [[CrossRef](#)]
29. Shao, C.Y.; Secombes, C.J.; Porter, A.J. Rapid isolation of IgNAR variable single-domain antibody fragments from a shark synthetic library. *Mol. Immunol.* **2007**, *44*, 656–665. [[CrossRef](#)]
30. Griffiths, K.; Dolezal, O.; Parisi, K.; Angerosa, J.; Dogovski, C.; Barraclough, M.; Sanalla, A.; Casey, J.; González, I.; Perugini, M.; et al. Shark Variable New Antigen Receptor (VNAR) Single Domain Antibody Fragments: Stability and Diagnostic Applications. *Antibodies* **2013**, *2*, 66–81. [[CrossRef](#)]
31. Liu, J.L.; Zabetakis, D.; Brown, J.C.; Anderson, G.P.; Goldman, E.R. Thermal stability and refolding capability of shark derived single domain antibodies. *Mol. Immunol.* **2014**, *59*, 194–199. [[CrossRef](#)] [[PubMed](#)]
32. Locksley, R.M.; Killeen, N.; Lenardo, M.J. The TNF and TNF receptor superfamilies: Integrating mammalian biology. *Cell* **2001**, *104*, 487–501. [[CrossRef](#)]
33. Lai, Y.; Dong, C. Therapeutic antibodies that target inflammatory cytokines in autoimmune diseases. *Int. Immunol.* **2016**, *28*, 181–188. [[CrossRef](#)] [[PubMed](#)]
34. Aggarwal, B.B. Signaling pathways of the TNF superfamily: A double-edged sword. *Nat. Rev. Immunol.* **2003**, *3*, 745–756. [[CrossRef](#)] [[PubMed](#)]
35. Caporali, R.; Crepaldi, G.; Codullo, V.; Benaglio, F.; Monti, S.; Todoerti, M.; Montecucco, C. 20 years of experience with tumour necrosis factor inhibitors: What have we learned? *Rheumatology* **2018**, *57*, vii5–viii10. [[CrossRef](#)]
36. Minozzi, S.; Bonovas, S.; Lytras, T.; Pecoraro, V.; Gonzalez-Lorenzo, M.; Bastiampillai, A.J.; Gabrielli, E.M.; Lonati, A.C.; Moja, L.; Cinquini, M.; et al. Risk of infections using anti-TNF agents in rheumatoid arthritis, psoriatic arthritis, and ankylosing spondylitis: A systematic review and meta-analysis. *Expert Opin. Drug Saf.* **2016**, *15*, 11–34. [[CrossRef](#)]
37. Callhoff, J.; Weiss, A.; Zink, A.; Listing, J. Impact of biologic therapy on functional status in patients with rheumatoid arthritis—A meta-analysis. *Rheumatology* **2013**, *52*, 2127–2135. [[CrossRef](#)]
38. Cohen, B.L.; Sachar, D.B. Update on anti-tumor necrosis factor agents and other new drugs for inflammatory bowel disease. *BMJ* **2017**, *357*, j2505. [[CrossRef](#)]
39. Thalayasingam, N.; Isaacs, J.D. Anti-TNF therapy. *Best Pract. Res. Clin. Rheumatol.* **2011**, *25*, 549–567. [[CrossRef](#)]
40. Udalova, I.; Monaco, C.; Nanchahal, J.; Feldmann, M. Anti-TNF Therapy. *Microbiol. Spectr.* **2016**, *4*, 46. [[CrossRef](#)]
41. Wang, X.; Li, F.; Qiu, W.; Xu, B.; Li, Y.; Lian, X.; Yu, H.; Zhang, Z.; Wang, J.; Li, Z.; et al. SYNBP: Synthetic binding proteins for research, diagnosis and therapy. *Nucleic Acids Res.* **2022**, *50*, D560–D570. [[CrossRef](#)] [[PubMed](#)]
42. Bojalil, R.; Mata-Gonzalez, M.T.; Sanchez-Munoz, F.; Yee, Y.; Argueta, I.; Bolanos, L.; Amezcua-Guerra, L.M.; Camacho-Villegas, T.A.; Sanchez-Castrejon, E.; Garcia-Ubbelohde, W.J.; et al. Anti-tumor necrosis factor VNAR single domains reduce lethality and regulate underlying inflammatory response in a murine model of endotoxic shock. *BMC Immunol.* **2013**, *14*, 17. [[CrossRef](#)] [[PubMed](#)]
43. Pepple, K.L.; Wilson, L.; Van Gelder, R.N.; Kovaleva, M.; Ubah, O.C.; Steven, J.; Barelle, C.J.; Porter, A. Uveitis Therapy With Shark Variable Novel Antigen Receptor Domains Targeting Tumor Necrosis Factor Alpha or Inducible T-Cell Costimulatory Ligand. *Transl. Vis. Sci. Technol.* **2019**, *8*, 11. [[CrossRef](#)] [[PubMed](#)]

44. Ubah, O.C.; Steven, J.; Kovaleva, M.; Ferguson, L.; Barelle, C.; Porter, A.J.R.; Barelle, C.J. Novel, Anti-hTNF-alpha Variable New Antigen Receptor Formats with Enhanced Neutralizing Potency and Multifunctionality, Generated for Therapeutic Development. *Front Immunol.* **2017**, *8*, 1780. [[CrossRef](#)] [[PubMed](#)]
45. Jumper, J.; Evans, R.; Pritzel, A.; Green, T.; Figurnov, M.; Ronneberger, O.; Tunyasuvunakool, K.; Bates, R.; Zidek, A.; Potapenko, A.; et al. Highly accurate protein structure prediction with AlphaFold. *Nature* **2021**, *596*, 583–589. [[CrossRef](#)]
46. Weng, G.; Wang, E.; Wang, Z.; Liu, H.; Zhu, F.; Li, D.; Hou, T. HawkDock: A web server to predict and analyze the protein-protein complex based on computational docking and MM/GBSA. *Nucleic Acids Res.* **2019**, *47*, W322–W330. [[CrossRef](#)]
47. Alford, R.F.; Leaver-Fay, A.; Jeliaskov, J.R.; O'Meara, M.J.; DiMaio, F.P.; Park, H.; Shapovalov, M.V.; Renfrew, P.D.; Mulligan, V.K.; Kappel, K.; et al. The Rosetta All-Atom Energy Function for Macromolecular Modeling and Design. *J. Chem. Theory Comput.* **2017**, *13*, 3031–3048. [[CrossRef](#)]
48. Beirnaert, E.; Desmyter, A.; Spinelli, S.; Lauwereys, M.; Aarden, L.; Dreier, T.; Loris, R.; Silence, K.; Pollet, C.; Cambillau, C.; et al. Bivalent Llama Single-Domain Antibody Fragments against Tumor Necrosis Factor Have Picomolar Potencies due to Intramolecular Interactions. *Front Immunol.* **2017**, *8*, 867. [[CrossRef](#)]
49. Dooley, H.; Flajnik, M.F. Shark immunity bites back: Affinity maturation and memory response in the nurse shark, *Ginglymostoma cirratum*. *Eur. J. Immunol.* **2005**, *35*, 936–945. [[CrossRef](#)]
50. Flajnik, M.F.; Dooley, H. The generation and selection of single-domain, v region libraries from nurse sharks. *Methods Mol. Biol.* **2009**, *562*, 71–82. [[CrossRef](#)]
51. Crouch, K.; Smith, L.E.; Williams, R.; Cao, W.; Lee, M.; Jensen, A.; Dooley, H. Humoral immune response of the small-spotted catshark, *Scyliorhinus canicula*. *Fish Shellfish Immunol.* **2013**, *34*, 1158–1169. [[CrossRef](#)] [[PubMed](#)]
52. Leow, C.H.; Fischer, K.; Leow, C.Y.; Braet, K.; Cheng, Q.; McCarthy, J. Isolation and characterization of malaria PfHRP2 specific VNAR antibody fragments from immunized shark phage display library. *Malar J.* **2018**, *17*, 383. [[CrossRef](#)] [[PubMed](#)]
53. Mirdita, M.; Steinegger, M.; Soding, J. MMseqs2 desktop and local web server app for fast, interactive sequence searches. *Bioinformatics* **2019**, *35*, 2856–2858. [[CrossRef](#)] [[PubMed](#)]
54. Baeyens, K.J.; De Bondt, H.L.; Raeymaekers, A.; Fiers, W.; De Ranter, C.J. The structure of mouse tumour-necrosis factor at 1.4 Å resolution: Towards modulation of its selectivity and trimerization. *Acta Crystallogr. D Biol. Crystallogr.* **1999**, *55*, 772–778. [[CrossRef](#)]
55. Du, Q.; Qian, Y.; Xue, W. Cross-reactivity of two human IL-6 family cytokines OSM and LIF explored by protein-protein docking and molecular dynamics simulation. *Biochim. Biophys. Acta Gen Subj.* **2021**, *1865*, 129907. [[CrossRef](#)]
56. Du, Q.; Qian, Y.; Xue, W. Molecular Simulation of Oncostatin M and Receptor (OSM-OSMR) Interaction as a Potential Therapeutic Target for Inflammatory Bowel Disease. *Front Mol. Biosci.* **2020**, *7*, 29. [[CrossRef](#)]
57. Yang, J.; Zhang, Z.; Yang, F.; Zhang, H.; Wu, H.; Zhu, F.; Xue, W. Computational design and modeling of nanobodies toward SARS-CoV-2 receptor binding domain. *Chem. Biol. Drug Des.* **2021**, *98*, 1–18. [[CrossRef](#)]
58. Chaudhury, S.; Berrondo, M.; Weitzner, B.D.; Muthu, P.; Bergman, H.; Gray, J.J. Benchmarking and analysis of protein docking performance in Rosetta v3.2. *PLoS ONE* **2011**, *6*, e22477. [[CrossRef](#)]